
HabiCrowd: A High Performance Simulator for Crowd-Aware Visual Navigation

An Dinh Vuong
FPT AI Center
Vietnam

Toan Tien Nguyen
FPT AI Center
Vietnam

Minh Nhat VU
TU Wien
Austria

Baoru Huang
Imperial College London/UCL
UK

Dzung Nguyen
FPT AI Center
Vietnam

Huynh Thi Thanh Binh
HUST
Vietnam

Thieu Vo
FPT AI Center
Vietnam

Anh Nguyen
University of Liverpool
UK

Abstract

Visual navigation, a foundational aspect of Embodied AI (E-AI), has been significantly studied in the past few years. While many 3D simulators have been introduced to support visual navigation tasks, scarcely works have been directed towards combining human dynamics, creating the gap between simulation and real-world applications. Furthermore, current 3D simulators incorporating human dynamics have several limitations, particularly in terms of computational efficiency, which is a promise of E-AI simulators. To overcome these shortcomings, we introduce HabiCrowd, the first standard benchmark for crowd-aware visual navigation that integrates a crowd dynamics model with diverse human settings into photorealistic environments. Empirical evaluations demonstrate that our proposed human dynamics model achieves state-of-the-art performance in collision avoidance, while exhibiting superior computational efficiency compared to its counterparts. We leverage HabiCrowd to conduct several comprehensive studies on crowd-aware visual navigation tasks and human-robot interactions. The source code and data can be found at <https://habicrowd.github.io/>.

1 Introduction

Embodied AI (E-AI), the intersection between computer vision, machine learning, and robotics, has gained interest amongst scientists in the past few years [22]. Training E-AI agents that can perceive, reason, and interact with the environment offers significant potential for sim2real applications [60]. The progress in E-AI research has been rapidly accelerated [71] thanks to the developments of fast and high-fidelity 3D simulators [68] that enable large-scale computational parallelization [59]. Among all E-AI studies, one of the most fundamental problems is visual navigation [26], which involves training an agent to navigate to a given goal using perception from the sensory inputs [49]. While many benchmarks have been proposed to address the visual navigation tasks in computer vision [68, 50, 12, 6, 13], most of them assume that navigating environments are static and do not consider human dynamics. Conversely, agents typically interact within dynamic environments, particularly those featuring humans whose positions constantly change [73]. If robots are to efficiently assist humans in routine duties, they must possess the capability to navigate effectively in *crowded and dynamic environments* [46]. Therefore, human dynamics is an essential factor that needs to be

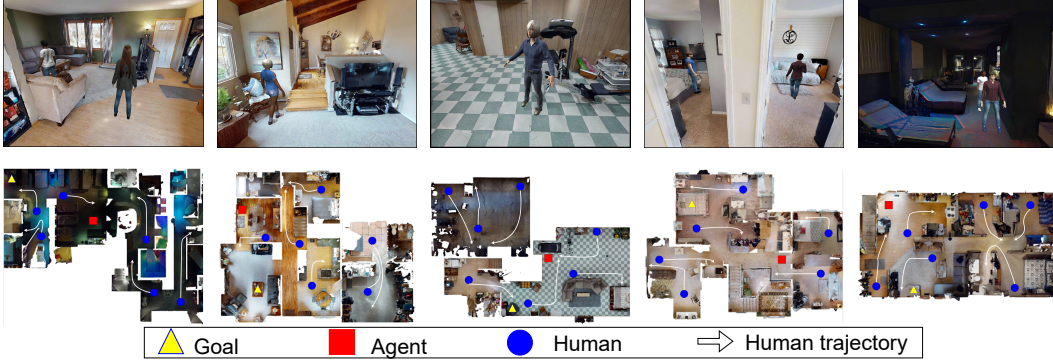


Figure 1: We present HabiCrowd, a new benchmark for crowd-aware visual navigation. The top row shows some example scenes, and the bottom row shows the floor plan with human dynamics.

thoroughly examined when developing E-AI benchmarks [8]. In this paper, we explore the tasks of visual navigation for an agent in the presence of human dynamics, aiming to bridge the gap between simulation and real-life scenarios.

The visual navigation task with the inclusion of human dynamics is widely referred to as the crowd-aware visual navigation task in the robotics community [14]. This task is challenging for several reasons. Firstly, to complete the navigation task, the agent needs to learn the patterns of human actions [34], which are complex and unstructured [21]. Furthermore, it is infeasible to predict the motion dynamics in crowded habitats as the motion of each person is typically affected by their neighbours [2]. Most prior works on crowd-aware navigation works in robotics usually consider training the agent in 2D simulators [14, 9, 34, 1, 15, 47, 23, 2, 64, 48, 39, 7]. The assumption of using 2D simulators is impractical [21] given that real-life robots primarily perceive human activities through visual sensors rather than employing mathematical social force models [71] to address the task.

Recently, a few attempts to add dynamic humans to 3D photorealistic simulators [36, 43] are shown to have limitations regarding the human dynamics model, as well as the available number of human models and scenes. In addition, one of the most critical drawbacks of recent 3D simulators integrating human dynamics lies in their computational efficiency. While E-AI simulators strive to facilitate rapid rendering and parallelization, prior simulators have proved to be inefficient in terms of computation [74, 43]. In general, the lack of 3D simulators with well-designed human dynamics makes the developed methods less applicable and expresses the necessity of establishing a standardized 3D benchmark for simulators that integrate human behaviors.

Motivated by these shortcomings, in this work, we introduce **HabiCrowd**, a new benchmark for the crowd-aware visual navigation task. HabiCrowd includes comprehensive social force-based human dynamics with diverse density settings operating in a large number of high-fidelity scenes from the Habitat-Matterport 3D dataset (HM3D) [52]. To assess the performance of HabiCrowd, several experiments are conducted, including benchmarking the human dynamics model, rendering speed, and memory utilization. Experimental results reveal that HabiCrowd achieves collision-free while running significantly faster than the state-of-the-art human dynamics model. Additionally, our HabiCrowd also exhibits a remarkable advantage in rendering speed and memory utilization compared to other related benchmarks. Upon HabiCrowd, we propose a new metric for crowd-aware navigation and benchmark two visual navigation tasks. The outcomes highlight the importance of human dynamics in navigating procedures. We also demonstrate that our new simulator enables various studies regarding human density and human-robot interactions. Our contributions are summarized as follows:

- We present HabiCrowd, a new dataset and benchmark for crowd-aware visual navigation. Experiments show that our simulator achieves a remarkable level of collision avoidance while surpassing other benchmarks in terms of human diversity and computational utilization.
- We benchmark navigation tasks on HabiCrowd and illustrate that our proposed simulator offers several in-depth analyses, such as studies of the impact of human density, human-robot avoidance, and human recognition on crowd-aware visual navigation tasks.

2 Related Works

Visual Navigation. Traditionally, roboticists have addressed visual navigation tasks by utilizing control methods such as Model Predictive Control (MPC) [56, 27]. Several following works have been proposed to improve control-based methods [58, 11, 3, 38, 75, 67]. The idea of control methods has been conserved by utilizing the advantage of deep learning [57, 20, 30, 6, 26, 24, 27]. Nevertheless, control-based methods demand a dynamics model and are often saturated when the number of ambiguities and the prediction horizon grows [41]. Recently, achievements in reinforcement learning (RL) [44] have brought about a significant shift in visual navigation [72]. Over the years, deep RL approaches have emerged as a widely adopted solution for addressing visual navigation tasks [68, 5, 42, 53, 28, 70, 31, 55], and many RL-based methods have achieved state-of-the-art results in visual navigation tasks such as point-goal navigation [68], object-goal navigation [54], image-goal navigation [70].

Crowd-aware Navigation. Navigation in crowded circumstances has significantly been examined by the robotics community [14]; however, most works only employ 2D simulators or small-scale experiment setups [35]. Earlier methods in crowd-aware navigation are primarily based on predicting the trajectories of human entities [9, 7, 23]. As the number of humans grows, the environment becomes exponentially denser; consequently, these trajectory-based approaches often suffer from the well-known freezing robot problem [63]. Learning-based methods have been introduced to overcome the freezing robot issue by automatically determining optimal waypoints [39]. Following this idea, RL frameworks are widely adopted to perceive human behaviors and interactions in a latent mechanism [14, 34, 1, 15, 2, 64, 40]. However, RL methods based on 2D simulators often suppose that the dynamics of all human entities are explicit and well-determined while the real-life interactions and human dynamics are much more arbitrary and complex [64]. To address this limitation, we study crowd-aware navigation in 3D settings, wherein the agent can only perceive the environment through egocentric inputs instead of 2D floor plans with known human dynamics.

3D Simulators for Visual Navigation. There have been a large number of simulators for the tasks of visual navigation [60, 45]. Gazebo, introduced in [32], is one of the first steps towards virtualizing the real world. Followed by Gazebo, several simulators have been established to study daily-conventional behaviors of robots, such as UnrealCV [51], AI2-THOR [33], Gibson [69], Habitat [59, 61]. Although the mentioned simulators provide opportunities to study interactions with humans, none of them have yet included human dynamics until the establishment of iGibson-Social Navigation (iGibson-SN) [36, 37]. More recently, Isaac Sim [43] is also established with the inclusion of virtual humans to the scenes. Nevertheless, the main drawbacks of both iGibson-SN and Isaac Sim are they have a limited number of scenes and human models. They also lack a measurement for crowdedness, which is an important factor in crowd-aware navigation problems [29]. With that inspiration, we propose a human dynamics model that is carefully designed and included in Habitat 2.0 [61] to create a standard and diverse crowd-aware visual navigation benchmark that closely reflects real-world conditions. Table 1 indicates the main differences between our HabiCrowd, iGibson Social Navigation (iGibson-SN), and Isaac Sim simulator. The comparisons highlight that our simulator offers a greater range of navigation settings, scenes, and human models.

	Dynamics model	Navigation settings	Num. scenes	Environment type	Num. humans	Crowdedness measurement
iGibson-SN [36]	ORCA [65]	Point-goal	15	residence	3	✗
Isaac Sim [43]	✗	Point-goal	7	office, warehouse traffic, hospital	7	✗
HabiCrowd (ours)	UPL++	Point-goal Object-goal	56	residence, gym, office, studio, club, restaurant	40	Human density

Table 1: **Comparison with related simulators.** We use the default settings [16] of Isaac Sim to benchmark scenes and virtual humans.

3 The HabiCrowd Simulator

In this section, we present HabiCrowd, a crowd-aware visual navigation simulator utilizing Habitat 2.0 [61] as the foundational simulator. The motivation behind this choice comes from the diverse environment settings and photorealistic scenes offered by Habitat 2.0 [71]. By integrating human dynamics into this simulator, HabiCrowd could further bridge the gap between simulation and real-life scenarios. Furthermore, Habitat 2.0 also enables parallel computing utilization [18], which could significantly facilitate the training procedure. We specify the configurations, trajectories, and controls of human dynamics of HabiCrowd.

3.1 Human Dynamics Model

We design a continuous and force-based human dynamics model, which progresses concurrently with the agent’s navigation, based on the universal power law (UPL) dynamics model proposed by [29]. Previously, UPL lacks the inclusion of torque components to control the facing direction of humans. To address this limitation, we further incorporate the torque dynamics model into the simulator. Consequently, our improved dynamics model is denoted as UPL++.

Assume the agent is navigating in a scene Λ with the set of obstacles W_Λ and n humans. We represent each human by $\mathbf{P}_i = (\mathbf{x}_i, \mathbf{v}_i, \hat{\mathbf{e}}_i, v_i, \psi_i, \psi_i^0, \omega_i, \omega_i^0, r_i, m_i)$ and consider their movements as particle kinematics on the 2D floor \mathbf{F} of Λ . Table 2 explains the notations in this section. Each \mathbf{P}_i will try to navigate to a destination \mathbf{d}_i . The model of \mathbf{P}_i is depicted in Figure 2.

Force Model. We utilize a force model for human entities to orient them to their destinations while minimizing collisions. The force model of \mathbf{P}_i projecting on \mathbf{F} can be written as:

$$\mathbf{f}_i = \mathbf{f}_i^{\text{adj}} + \sum_{j=1, j \neq i}^n (\mathbf{f}_{i,j}^{\text{soc}} + \mathbf{f}_{i,j}^{\text{con}}) + \sum_{w \in W_\Lambda} \mathbf{f}_{i,w}^{\text{con}} + \zeta_i. \quad (1)$$

The fluctuation force $\zeta_i = \zeta'_i \vec{n}(\varphi_i)$ is included to break the symmetry of all humans, where $\zeta'_i \sim \mathcal{N}(0, \sigma_\zeta^2)$, $\varphi_i \sim \mathcal{U}(0, 2\pi)$, and $\vec{n}(\varphi_i)$ is the unit vector rotated by φ_i about the origin of \mathbf{F} .

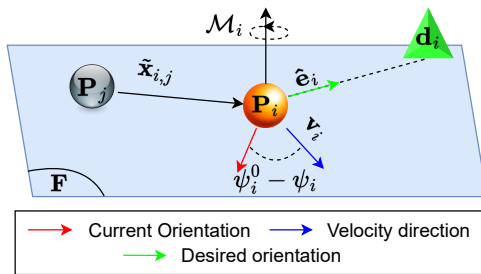


Figure 2: Human dynamics model. We design a model to shape \mathbf{P}_i towards \mathbf{d}_i while avoiding collisions with \mathbf{P}_j . The human dynamics includes a force model and a torque model.

Not.	Description
r_i	Particle's radius
$\hat{\mathbf{e}}_i$	Desired direction
\mathbf{x}_i	Human coordinate
\mathbf{v}_i	Linear velocity
v_i	Desired velocity
m_i	Human mass
ω_i	Current angular velocity
ω_i^0	Desired angular velocity
ψ_i	Angular coordinate of the current orientation
ψ_i^0	Angular coordinate of the desired orientation

Table 2: **Notations of human dynamics.**

The contact force $\mathbf{f}_{i,*}^{\text{con}}$, which is a consequence of a collision between other entities like objects/humans, indicates the corresponding physical reaction. In the former notation, $*$ is a placeholder indicating either an obstacle w or another human index j . We rely on the core physic engine of Habitat 2.0, PyBullet [17] to model the contact force.

The adjust force $\mathbf{f}_i^{\text{adj}}$ shapes the agent to navigate towards its destination \mathbf{d}_i . Specifically, $\mathbf{f}_i^{\text{adj}} = m_i / \tau^{\text{adj}} (v_i \hat{\mathbf{e}}_i - \mathbf{v}_i)$, where τ^{adj} is the characteristic time of adjusting force.

Finally, we establish the social force model between \mathbf{P}_i and \mathbf{P}_j to prolong their time-to-collision based on their linearly-estimated positions. Let τ be the time-to-collision between two entities and

$\tilde{\mathbf{x}}, \tilde{\mathbf{v}}$ be their relative position and velocity, respectively. Inspired by [29], we define the interaction energy between \mathbf{P}_i and \mathbf{P}_j , as follows:

$$E(\tau) = \frac{k^{\text{soc}}}{\tau^2} \exp\left(-\frac{\tau}{\tau^{\text{soc}}}\right), \quad (2)$$

where k^{soc} is a value for adjusting social force, τ^{soc} is the interaction time horizon. The skin-to-skin distance h between two human entities after τ is given by $h(\tau) = \|\tilde{\mathbf{x}} + \tau\tilde{\mathbf{v}}\|_2 - (r_i + r_j)$.

Intuitively, the collision occurs when the skin-to-skin distance zeros; therefore, by solving the quadratic equation $h(\tau) = 0$, we obtain τ as:

$$\tau(\tilde{\mathbf{x}}) = \frac{b - \sqrt{b^2 - ac}}{a}, \quad (3)$$

where $a = \|\tilde{\mathbf{v}}\|_2^2$; $b = -\tilde{\mathbf{x}}^\top \tilde{\mathbf{v}}$; $c = \|\tilde{\mathbf{x}}\|_2^2 - (r_i + r_j)^2$. Following [29], we calculate the desired social force as $\mathbf{f}_{i,j}^{\text{soc}}(\tilde{\mathbf{x}}) = -\nabla_{\tilde{\mathbf{x}}} E(\tau)$.

Torque Model. We design a torque model to keep the orientation of \mathbf{P}_i coinciding with the direction of \mathbf{v}_i . We denote $I_i = m_i r_i^2$ as the \mathbf{P}_i 's moment of inertia. Then, the torque is formulated as follows:

$$\mathcal{M}_i = \mathcal{M}_i^{\text{adj}} + \sum_{j=1, j \neq i}^n \mathcal{M}_{i,j}^{\text{con}} + \sum_{w \in W_\Lambda} \mathcal{M}_{i,w}^{\text{con}} + \eta_i. \quad (4)$$

The fluctuation torque $\eta_i \sim \mathcal{N}(0, \sigma_\eta^2)$ aims to break the crowd symmetry by randomly altering \mathbf{P}_i 's orientation.

The contact torque $\mathcal{M}_{i,*}^{\text{con}}$ is also based on the foundation simulator, which is similar to $\mathbf{f}_{i,*}^{\text{con}}$.

The adjusting torque shapes the orientation of the human entity towards its desired orientation, which is the current linear velocity \mathbf{v}_i (see Figure 2). Additionally, we want to keep the angular velocity at a reasonable rate ω_i^0 . As a consequence, we design the adjusting torque as follows:

$$\mathcal{M}_i^{\text{adj}} = \frac{I_i}{\tau^{\text{rot}}} \left[\left(\frac{(\psi_i^0 - \psi_i) \bmod 2\pi}{\pi} - 1 \right) \omega_i^0 - \omega_i \right], \quad (5)$$

where τ^{rot} is the characteristic time of adjusting torque.

Computational Complexity. We determine the computational complexity for the i -th virtual human. It can be implied from Eqs. (1) and (4) that the computation complexity for \mathbf{f}_i and \mathcal{M}_i is both $O(n)$. This is because, apart from $\mathbf{f}_{i,j}^{\text{soc}}$ and $\mathbf{f}_{i,j}^{\text{con}}$, which require $O(n)$ computations, the remaining components only need constant computations.

We note that our UPL++ dynamics model and ORCA [65] that is used in iGibson-SN [36] share the same computational complexity of $O(n)$. However, the major difference between our UPL++ and ORCA is the approach used to determine the dynamic terms, \mathbf{f}_i and \mathcal{M}_i . While UPL++ directly computes these terms, ORCA employs an indirect approach by solving an LP problem. Empirical results in Section 4.1 confirm that the constant factor associated with UPL++ is considerably smaller than ORCA's, indicating a computational efficiency advantage in favor of UPL++.

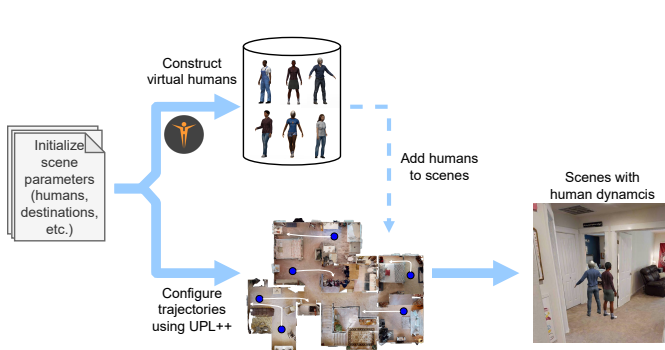


Figure 3: Dataset construction pipeline.

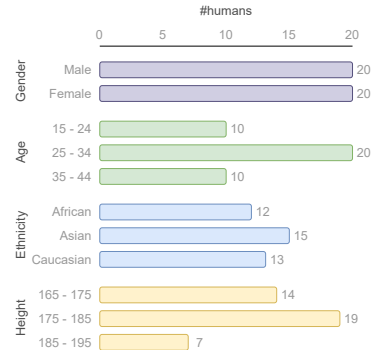


Figure 4: Human statistics.

3.2 Dataset Construction

Figure 3 illustrates the pipeline to build HabiCrowd scenes. We begin with initializing parameters for each virtual human P_i and their destination d_i . Next, we construct virtual humans using the MakeHuman [10]. Then the trajectories of humans are configured by using the dynamics model in Section 3.1 and are added to the scenes of HM3D dataset [52] to create the final scenes. Note that when a human entity reaches its destination, we navigate it back to its original position and repeat this loop to maintain human dynamics during the agent’s navigation.

Dataset Statistics. We utilize 56 scenes from HM3D [52] and 40 human entities. The train/val/test splits are 36/8/12. HabiCrowd’s virtual humans have a gender ratio of 1/1 and ages range from 15 to 44 (Figure 4). The human density and navigation area distributions are depicted in Figure 5. Our simulator provides a broad spectrum of navigation settings including different levels of human density, spanning from 0.1 to 0.5, as well as navigation areas ranging from 10m² to 300m². The average human density of HabiCrowd is 0.189 humans per m², which is close to 0.143, the real crowd density in the real world [19]. Our simulator also has scenes with higher density (for example, 0.45) to make the problem more challenging.

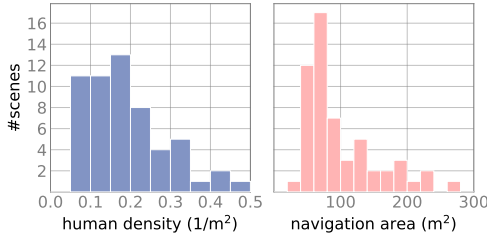


Figure 5: Navigating statistics.

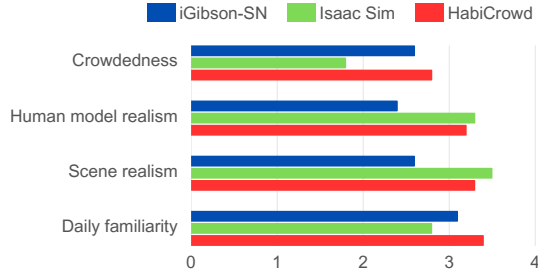


Figure 6: User evaluation.

4 Experiments

4.1 HabiCrowd Evaluation

Performance and Memory Benchmarks. Figure 7 compares the average rendering speed (frame per second - FPS) and memory (RAM) utilization for each scene among three simulators. The process is conducted over a set of 6 scenes of each simulator on a cluster of 4 RTX 3090 GPUs. We observe a downward trend in FPS and an upward trend in memory usage for all simulators as the number of virtual humans within the scenes increases. These phenomena are primarily due to the saturation of computational complexity when more humans are added to the scenes. Nevertheless, our HabiCrowd consistently exhibits an average FPS that is nearly three times higher than iGibson-SN’s and two times higher than Isaac Sim’s. Furthermore, in terms of memory efficiency, both our simulator and iGibson-SN stand out by requiring less than 400 MB of RAM to render each scene. In contrast, Isaac Sim necessitates over 2560 MB of RAM to render scenes with high fidelity. To conclude, our proposed simulator achieves the most efficient computational utilization compared to other baselines.

Human Dynamics Evaluation. We utilize the UMANS engine [66] to compare our HabiCrowd dynamic model UPL++ with ORCA dynamic model in iGibson-SN on the following aspects: *i*) Average computational time (mCT): determines the average computational time that each dynamics model needs to update the state for each virtual human during the navigation process. *ii*) Collision avoidance rate (CAR): measures how many times collisions between virtual humans are avoided. *iii*) Goal-reaching rate (GR): computes the frequency of virtual humans navigating to their destinations.

Table 3 reports the evaluation results. This table shows that both iGibson-SN and our simulator achieve collision-free navigation. Although HabiCrowd demonstrates a goal-reaching rate comparable to iGibson-SN’s (with a slight margin of 0.78%), our model shows remarkable improvement in terms of computational time, which is *nearly twice faster* than iGibson-SN.

Recall from Section 3.1 that the computational complexity of iGibson-SN and HabiCrowd is $O(n)$. However, from Figure 9, we observe that the slope of HabiCrowd is considerably steeper than iGibson-SN’s, indicating that the corresponding constant factor of HabiCrowd is significantly smaller than its

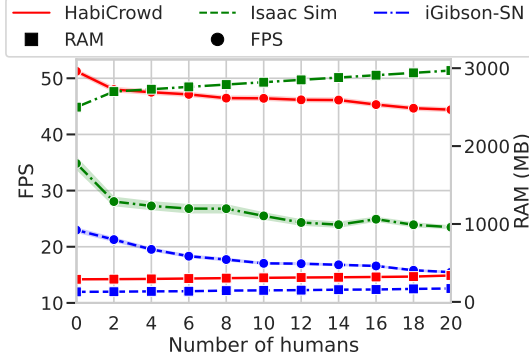


Figure 7: **Performance and memory benchmarks.**

counterpart. As a result, the computational efficiency advantage of HabiCrowd over iGibson-SN is preserved even when the number of humans scales up.

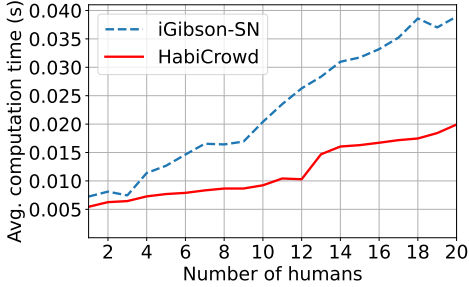


Figure 9: **Average computational time of human dynamics.**

User Study. We provide a user study with 28 participants and ask them to rate HabiCrowd, Isaac Sim, and iGibson-SN on four criteria: crowdedness, human model realism, scene realism, and daily familiarity. Figure 6 shows that in all aspects, our simulator is preferred over iGibson-SN. Moreover, our simulator exhibits comparable metrics in terms of human model realism and scene realism compared to Isaac Sim. Our provided environments are also considered to be more crowded and daily familiar than Isaac Sim.

Human Poses Comparison. We extract human poses from all datasets by using the PCT approach [25] and provide the qualitative analysis in Figure 8. The findings reveal that our simulator showcases a greater degree of diversity in human poses when compared to the other simulators. Consequently, HabiCrowd captures a wider range of human pose variations, therefore, reflecting a more comprehensive representation of real-life human settings.

4.2 Crowd-aware Visual Navigation

Experimental Settings. We examine two crowd-aware visual navigation tasks upon HabiCrowd, namely, *point navigation* [68] and *object navigation* [12]. The agent is initialized at a pre-defined location in a human-crowded scene and asked to navigate to an objective. At each timestep, the agent receives RGB and depth images that depict its egocentric viewpoint. We introduce an additional objective that requires the agent to minimize the frequency of collisions with virtual humans. Each collision is counted when the skin-to-skin distance between the agent and any human zeros.

Denote d_t as the distance from the agent to the goal at timestep t , we design the reward model as: $r_t = R^c \mathbb{I}_t^c + R^s \mathbb{I}_t^s + R^f \times (d_t - d_{t-1})$, where R^c is the collision penalty, R^s is the reward for completing the task, R^f is the shaping reward for moving closer to the objective, and $\mathbb{I}_t^c, \mathbb{I}_t^s$ are the indicators of collision and success of the current step, respectively. This reward model helps balance between navigating towards the objective and avoiding collisions. We train all methods using the above reward model. Followed by [12], we set $R^s = 2.5, R^f = 1.0$. The default value of R^c is set to -10^{-4} . For the human dynamics, we set $\tau^{\text{adj}} = 0.5, \tau^{\text{soc}} = 3.0, \tau^{\text{rot}} = 0.2$ and $k^{\text{soc}} = 1.5$ in all

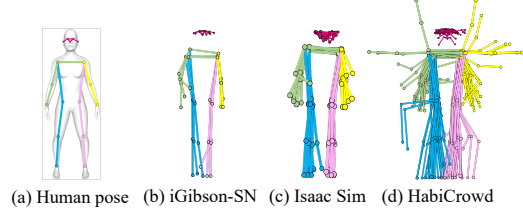


Figure 8: **Human poses comparison.** Our normalization process ensures that all human poses have the upper body facing the front (a).

setups. Each method is trained in an end-to-end fashion using a total of 30M frames. We run each experiment on a computing cluster utilizing a node of four 48GB-RAM V100 GPUs.

Baselines. We compare the following baselines: *i)* DS-RNN [39]: A spatial and temporal learning-based agent. *ii)* DD-PPO [68]: A widely-used state-of-the-art optimization algorithm in E-AI tasks. *iii)* LB-WPN [62]: A method that combines a learning-based perception module and a model-based planning module for autonomous navigation among humans. *iv)* DOA [74]: The winning entry of the 2021 iGibson-SN challenge [36] that applies the dynamic obstacle augmentation method. *v)* OVRL-v2 [70]: A recent state-of-the-art baseline utilizing the vision transformer approach (ViT).

Metrics. We employ three widely used metrics in traditional visual navigation tasks [12], namely, *i)* Distance to goal (DTG), *ii)* Success rate (SR - in %), *iii)* Success path length [4] (SPL - in %). Additionally, we introduce *iv)* **Collisions per distance (CPD)**, a new metric to quantify collisions occurring between the navigating agent and virtual humans. This metric is computed by dividing the number of collisions between the agent and humans by the distance traveled by the agent.

Point Navigation Results. We present the point navigation results in Table 4. Overall, every baseline achieves decent performance, OVRL-v2 achieves the most comprehensive performance in terms of all metrics. Since HabiCrowd does not provide dynamics information regarding virtual humans to the agent due to our aim of enabling more realistic navigation settings, baselines such as DS-RNN [39], LB-WPN [62] are unable utilize human dynamics models to address the task effectively. On the other hand, OVRL-v2 leverages ViT, a robust vision backbone capable of extracting entities (such as virtual humans) from visual inputs as additional clues, thereby proficiently handling the task.

	CPD ↓	SPL ↑	SR ↑	DTG ↓
LB-WPN [62]	0.0509	78.92	92.01	0.6136
DOA [74]	0.0694	80.59	92.42	0.5972
DD-PPO [68]	0.0526	77.64	92.21	0.5985
DS-RNN [39]	0.0427	76.21	90.88	0.6745
OVRL-v2 [70]	0.0295	82.78	94.68	0.4737

Table 4: **Point navigation results.** Experiments are conducted on HabiCrowd.

	CPD ↓	SPL ↑	SR ↑	DTG ↓
LB-WPN [62]	0.0381	3.410	6.457	6.746
DOA [74]	0.0342	3.483	7.209	6.417
DD-PPO [68]	0.0244	3.745	5.877	6.367
DS-RNN [39]	0.0168	3.030	6.043	6.668
OVRL-v2 [70]	0.0146	5.975	10.732	6.314

Table 5: **Object navigation results.** We evaluate all baselines on the proposed HabiCrowd.

Object Navigation Results. Table 5 illustrates the results on the HabiCrowd dataset by all approaches. It is obvious that object navigation poses a significantly greater challenge than point navigation, as evidenced by the decline in evaluation metrics for all baseline methods. The decrease in performance is aligned with the expectations outlined in [31]. The results show that OVRL-v2 has the best success rate, outperforming the second-best algorithm (DOA) by 3.523%.

How does human density affect crowd navigation? Table 6 shows the success rates when we test all methods with different human density setups. OVRL-v2 stably outperforms other algorithms by 2.679%, 1.758%, and a significant margin of 2.924% when the human density are from < 0.2 ; $0.2 - 0.3$; and > 0.3 , respectively. In general, we observe that the higher the human density, the more challenging our task becomes as the success rates obtained by all methods decrease.

Density	< 0.2	$0.2 - 0.3$	> 0.3
LB-WPN [62]	7.363	3.328	1.515
DOA [74]	8.416	4.337	2.201
DD-PPO [68]	8.135	6.064	2.525
DS-RNN [39]	7.854	5.051	2.530
OVRL-v2 [70]	11.095	7.822	5.454

Table 6: **Human density analysis.** We show object navigation success rates of all methods by different human density setups.



Figure 10: **Human attention.** We depict the attention mechanism used by ViT backbone of OVRL-v2.

Does our reward model help? Table 7 reports the results of when all baselines use our reward model and when they do not. Evidently, our reward model yields improved performance in terms of CPD, SPL, and SR across all methods. We explain as follows. The introduced quantity R^c contributes to agents' regularization towards avoiding collisions with virtual humans, consequently improving performances in unseen cases.

	Without our reward model				With our reward model											
	$R^c = 0.0$				$R^c = -10^{-4}$				$R^c = -10^{-3}$				$R^c = -10^{-2}$			
	CPD↓	SPL↑	SR↑	DTG↓	CPD↓	SPL↑	SR↑	DTG↓	CPD↓	SPL↑	SR↑	DTG↓	CPD↓	SPL↑	SR↑	DTG↓
LB-WPN [62]	0.043	3.81	7.11	6.36	0.038	3.41	6.46	6.75	0.029	1.76	3.97	6.64	0.021	2.15	0.73	7.12
DOA [74]	0.127	4.01	7.19	6.59	0.034	3.48	7.20	6.75	0.024	2.34	4.53	6.60	0.015	0.44	1.66	7.31
DD-PPO [68]	0.023	1.96	4.47	6.60	0.024	3.75	5.88	6.37	0.053	2.90	4.22	6.66	0.018	1.16	1.41	7.18
DS-RNN [39]	0.067	4.13	6.46	6.77	0.017	3.03	6.04	6.67	0.021	0.37	0.83	7.74	0.445	0.61	0.75	7.38
OVRL-v2 [70]	0.042	4.29	9.36	6.13	0.015	5.98	10.73	6.31	0.020	3.09	4.81	6.58	0.012	2.65	3.06	7.01

Table 7: **Impact of collision penalty.** We vary R^c and showcase the object navigation performance.

How does collision penalty affect crowd navigation? We study the impact of R^c on our navigation problem. We observe in Table 7 that starting from $R^c = -10^{-4}$ to -10^{-2} , all baselines experience a downward tendency in success rates and an upward tendency in collision avoidance. This observation is to be expected, considering that R^c serves as a regularizing factor for the collision avoidance component. Consequently, as R^c diminishes, the focus of the baselines shifts towards prioritizing collision avoidance with virtual humans rather than navigating towards the goal.

Will attention mechanism help? Figure 10 demonstrates how the attention mechanism works in ViT backbone of OVRL-v2. We can see that the agent trained with the transformer-based method learns to attend to virtual humans of the scene to extract more useful information to complete the navigation tasks. However, it is noticeable that ViT also allocates attention to image patches representing the wall and ceiling, indicating potential areas for improvements of the attention mechanism.

What is the drawback of current methods? A notable weakness of all current baselines is that they do not possess an *explicit* strategy to determine human dynamics from RGB-D egocentric observations. Although OVRL-v2 has a robust vision backbone to extract human dynamics information, the employed mechanism remains *implicit* and demands for improvements.

Discussion. From the experiments, we can see that the point-goal crowd-aware navigation task is well-addressed, while the object-goal task remains a challenge. We have highlighted the critical issue in 3D crowd-aware visual navigation tasks, emphasizing the necessity of explicitly extracting human dynamics solely from RGB-D observations. This direction should be studied as making efforts towards solving crowd-aware navigation in real-life settings, where robots can only perceive human behaviors via sensor inputs without the assumption of a known human dynamics model.

5 Conclusion and Future Work

We have presented HabiCrowd, a new crowd-aware simulator built upon Habitat 2.0. HabiCrowd has a robust human dynamic model and a diverse range of virtual humans compared to related simulators. The intensive experimental results indicate that our simulator utilizes computational resources more efficiently than its counterparts. We evaluate two visual navigation tasks and show that the recognition of virtual humans depicted in egocentric inputs is essential. Nevertheless, HabiCrowd still has limitations. While humans exhibit natural movements in daily lives, the constraints imposed by Habitat 2.0 [61] only allow for rigid movements. This assumption falls considerably behind the complexity of real-life practice and thus requires further enhancements. Finally, applying the learned policy from HabiCrowd to the real world remains an open problem for future work.

References

- [1] Alexandre Alahi, Kratharth Goel, Vignesh Ramanathan, Alexandre Robicquet, Li Fei-Fei, and Silvio Savarese. Social lstm: Human trajectory prediction in crowded spaces. In *Proceedings of the IEEE Conference on Computer Vision and Pattern Recognition*, 2016.
- [2] Alexandre Alahi, Vignesh Ramanathan, Kratharth Goel, Alexandre Robicquet, Amir A Sadeghian, Li Fei-Fei, and Silvio Savarese. Learning to predict human behavior in crowded scenes. In *Group and Crowd Behavior for Computer Vision*. Elsevier, 2017.
- [3] Guillaume Allibert, Estelle Courtial, and Youssoufi Touré. Real-time visual predictive controller for image-based trajectory tracking of a mobile robot. *IFAC Proceedings Volumes*, 2008.

- [4] Peter Anderson, Angel Chang, Devendra Singh Chaplot, Alexey Dosovitskiy, Saurabh Gupta, Vladlen Koltun, Jana Kosecka, Jitendra Malik, Roozbeh Mottaghi, Manolis Savva, et al. On evaluation of embodied navigation agents. *arXiv preprint arXiv:1807.06757*, 2018.
- [5] Andrea Banino, Caswell Barry, Benigno Uria, Charles Blundell, Timothy Lillicrap, Piotr Mirowski, Alexander Pritzel, Martin J Chadwick, Thomas Degris, Joseph Modayil, et al. Vector-based navigation using grid-like representations in artificial agents. *Nature*, 2018.
- [6] Somil Bansal, Varun Tolani, Saurabh Gupta, Jitendra Malik, and Claire Tomlin. Combining optimal control and learning for visual navigation in novel environments. In *Conference on Robot Learning*, 2020.
- [7] Maren Bennewitz, Wolfram Burgard, Grzegorz Cielniak, and Sebastian Thrun. Learning motion patterns of people for compliant robot motion. *The International Journal of Robotics Research*, 2005.
- [8] Francisco Bonin-Font, Alberto Ortiz, and Gabriel Oliver. Visual navigation for mobile robots: A survey. *Journal of Intelligent and Robotic Systems*, 2008.
- [9] Johann Borenstein and Yoram Koren. Real-time obstacle avoidance for fast mobile robots. *IEEE Transactions on Systems, Man, and Cybernetics*, 1989.
- [10] Leyde Briceno and Gunther Paul. Makehuman: A review of the modelling framework. In *Congress of the International Ergonomics Association*, 2018.
- [11] Berk Calli and Aaron M Dollar. Vision-based model predictive control for within-hand precision manipulation with underactuated grippers. In *IEEE International Conference on Robotics and Automation*, 2017.
- [12] Devendra Singh Chaplot, Dhiraj Prakashchand Gandhi, Abhinav Gupta, and Russ R Salakhutdinov. Object goal navigation using goal-oriented semantic exploration. *Advances in Neural Information Processing Systems*, 2020.
- [13] Changan Chen, Unnat Jain, Carl Schissler, Sebastia Vicenc Amengual Gari, Ziad Al-Halah, Vamsi Krishna Ithapu, Philip Robinson, and Kristen Grauman. Soundspaces: Audio-visual navigation in 3d environments. In *European Conference on Computer Vision*, 2020.
- [14] Changan Chen, Yuejiang Liu, Sven Kreiss, and Alexandre Alahi. Crowd-robot interaction: Crowd-aware robot navigation with attention-based deep reinforcement learning. In *IEEE International Conference on Robotics and Automation*, 2019.
- [15] Yu Fan Chen, Michael Everett, Miao Liu, and Jonathan P How. Socially aware motion planning with deep reinforcement learning. In *IEEE/RSJ International Conference on Intelligent Robots and Systems*, 2017.
- [16] NVIDIA Corporation. Nvidia omniverse platform for creating and operating metaverse applications, 2023. Accessed: May 15th 2023. [Online]. Available: <https://www.nvidia.com/en-us/omniverse/>.
- [17] Erwin Coumans and Yunfei Bai. Pybullet, a python module for physics simulation for games, robotics and machine learning, 2019. Accessed: April 25th 2023. [Online]. Available: <https://pybullet.org/wordpress/>.
- [18] Matt Deitke, Dhruv Batra, Yonatan Bisk, Tommaso Campari, Angel X Chang, Devendra Singh Chaplot, Changan Chen, Claudia Pérez D’Arpino, Kiana Ehsani, Ali Farhadi, et al. Retrospectives on the embodied ai workshop. *arXiv preprint arXiv:2210.06849*, 2022.
- [19] Drivers Jonas Deloitte. Employment densities guide, 2010. Accessed: May 29th 2023. [Online]. Available: https://assets.publishing.service.gov.uk/government/uploads/system/uploads/attachment_data/file/378203/employ-den.pdf.
- [20] Paul Drews, Grady Williams, Brian Goldfain, Evangelos A Theodorou, and James M Rehg. Aggressive deep driving: Combining convolutional neural networks and model predictive control. In *Conference on Robot Learning*, 2017.

- [21] Daniel Dugas, Olov Andersson, Roland Siegwart, and Jen Jen Chung. Navdreams: Towards camera-only rl navigation among humans. *arXiv preprint arXiv:2203.12299*, 2022.
- [22] Kiana Ehsani, Winson Han, Alvaro Herrasti, Eli VanderBilt, Luca Weihs, Eric Kolve, Aniruddha Kembhavi, and Roozbeh Mottaghi. Manipulathor: A framework for visual object manipulation. In *Proceedings of the IEEE/CVF Conference on Computer Vision and Pattern Recognition*, 2021.
- [23] Gonzalo Ferrer, Anaïs Garrell, and Alberto Sanfeliu. Robot companion: A social-force based approach with human awareness-navigation in crowded environments. In *IEEE/RSJ International Conference on Intelligent Robots and Systems*, 2013.
- [24] Chelsea Finn and Sergey Levine. Deep visual foresight for planning robot motion. In *IEEE International Conference on Robotics and Automation*, 2017.
- [25] Zigang Geng, Chunyu Wang, Yixuan Wei, Ze Liu, Houqiang Li, and Han Hu. Human pose as compositional tokens. In *Proceedings of the IEEE/CVF Conference on Computer Vision and Pattern Recognition*, 2023.
- [26] Saurabh Gupta, James Davidson, Sergey Levine, Rahul Sukthankar, and Jitendra Malik. Cognitive mapping and planning for visual navigation. In *Proceedings of the IEEE Conference on Computer Vision and Pattern Recognition*, 2017.
- [27] Noriaki Hirose, Fei Xia, Roberto Martín-Martín, Amir Sadeghian, and Silvio Savarese. Deep visual mpc-policy learning for navigation. *IEEE Robotics and Automation Letters*, 2019.
- [28] Tudor Jianu, Baoru Huang, Mohamed EMK Abdelaziz, Minh Nhat Vu, Sebastiano Fichera, Chun-Yi Lee, Pierre Berthet-Rayne, and Anh Nguyen. Cathsim: An open-source simulator for autonomous cannulation. *arXiv preprint arXiv:2208.01455*, 2022.
- [29] Ioannis Karamouzas, Brian Skinner, and Stephen J Guy. Universal power law governing pedestrian interactions. *Physical Review Letters*, 2014.
- [30] Elia Kaufmann, Antonio Loquercio, Rene Ranftl, Alexey Dosovitskiy, Vladlen Koltun, and Davide Scaramuzza. Deep drone racing: Learning agile flight in dynamic environments. In *Conference on Robot Learning*, 2018.
- [31] Apoorv Khandelwal, Luca Weihs, Roozbeh Mottaghi, and Aniruddha Kembhavi. Simple but effective: Clip embeddings for embodied ai. In *Proceedings of the IEEE/CVF Conference on Computer Vision and Pattern Recognition*, 2022.
- [32] Nathan Koenig and Andrew Howard. Design and use paradigms for gazebo, an open-source multi-robot simulator. In *IEEE/RSJ International Conference on Intelligent Robots and Systems*, 2004.
- [33] Eric Kolve, Roozbeh Mottaghi, Winson Han, Eli VanderBilt, Luca Weihs, Alvaro Herrasti, Daniel Gordon, Yuke Zhu, Abhinav Gupta, and Ali Farhadi. Ai2-thor: An interactive 3d environment for visual ai. *arXiv preprint arXiv:1712.05474*, 2017.
- [34] Henrik Kretzschmar, Markus Spies, Christoph Sprunk, and Wolfram Burgard. Socially compliant mobile robot navigation via inverse reinforcement learning. *The International Journal of Robotics Research*, 2016.
- [35] Thibault Kruse, Amit Kumar Pandey, Rachid Alami, and Alexandra Kirsch. Human-aware robot navigation: A survey. *Robotics and Autonomous Systems*, 2013.
- [36] Chengshu Li, Jaewoo Jang, Fei Xia, Roberto Martín-Martín, Claudia D’Arpino, Alexander Toshev, Anthony Francis, Edward Lee, and Silvio Savarese. iGibson Challenge 2021, 2021.
- [37] Chengshu Li, Jaewoo Jang, Fei Xia, Roberto Martín-Martín, Claudia D’Arpino, Alexander Toshev, Anthony Francis, Edward Lee, and Silvio Savarese. iGibson Challenge 2022, 2022.
- [38] Zhijun Li, Chenguang Yang, Chun-Yi Su, Jun Deng, and Weidong Zhang. Vision-based model predictive control for steering of a nonholonomic mobile robot. *IEEE Transactions on Control Systems Technology*, 2015.

- [39] Shuijing Liu, Peixin Chang, Weihang Liang, Neeloy Chakraborty, and Katherine Driggs-Campbell. Decentralized structural-rnn for robot crowd navigation with deep reinforcement learning. In *IEEE International Conference on Robotics and Automation*, 2021.
- [40] Shih-Yun Lo, Katsu Yamane, and Ken-ichiro Sugiyama. Perception of pedestrian avoidance strategies of a self-balancing mobile robot. In *IEEE/RSJ International Conference on Intelligent Robots and Systems*, 2019.
- [41] Sergio Lucia, Sankaranarayanan Subramanian, Daniel Limon, and Sebastian Engell. Stability properties of multi-stage nonlinear model predictive control. *Systems & Control Letters*, 2020.
- [42] Liulong Ma, Jiao Chen, et al. Using rgb image as visual input for mapless robot navigation. *arXiv preprint arXiv:1903.09927*, 2019.
- [43] Viktor Makoviychuk, Lukasz Wawrzyniak, Yunrong Guo, Michelle Lu, Kier Storey, Miles Macklin, David Hoeller, Nikita Rudin, Arthur Allshire, Ankur Handa, et al. Isaac gym: High performance gpu-based physics simulation for robot learning. *arXiv preprint arXiv:2108.10470*, 2021.
- [44] Volodymyr Mnih, Koray Kavukcuoglu, David Silver, Andrei A Rusu, Joel Veness, Marc G Bellemare, Alex Graves, Martin Riedmiller, Andreas K Fidjeland, Georg Ostrovski, et al. Human-level control through deep reinforcement learning. *Nature*, 2015.
- [45] Ronja Möller, Antonino Furnari, Sebastiano Battiato, Aki Härmä, and Giovanni Maria Farinella. A survey on human-aware robot navigation. *Robotics and Autonomous Systems*, 2021.
- [46] Gianluca Monaci, Michel Aractingi, and Tomi Silander. Dipcan: Distilling privileged information for crowd-aware navigation. *Robotics: Science and Systems (RSS) XVIII*, 2022.
- [47] Anh Nguyen, Tuong Do, Minh Tran, Binh X Nguyen, Chien Duong, Tu Phan, Erman Tjiputra, and Quang D Tran. Deep federated learning for autonomous driving. In *2022 IEEE Intelligent Vehicles Symposium (IV)*, 2022.
- [48] Anh Nguyen, Ngoc Nguyen, Kim Tran, Erman Tjiputra, and Quang D Tran. Autonomous navigation in complex environments with deep multimodal fusion network. In *2020 IEEE/RSJ International Conference on Intelligent Robots and Systems*, 2020.
- [49] Khanh Nguyen, Debadeepta Dey, Chris Brockett, and Bill Dolan. Vision-based navigation with language-based assistance via imitation learning with indirect intervention. In *Proceedings of the IEEE/CVF Conference on Computer Vision and Pattern Recognition*, 2019.
- [50] Khanh Nguyen and Hal Daumé III. Help, anna! visual navigation with natural multimodal assistance via retrospective curiosity-encouraging imitation learning. In *Conference on Empirical Methods in Natural Language Processing and International Joint Conference on Natural Language Processing*, 2019.
- [51] Weichao Qiu, Fangwei Zhong, Yi Zhang, Siyuan Qiao, Zihao Xiao, Tae Soo Kim, and Yizhou Wang. Unrealcv: Virtual worlds for computer vision. In *ACM International Conference on Multimedia*, 2017.
- [52] Santhosh K Ramakrishnan, Aaron Gokaslan, Erik Wijmans, Oleksandr Maksymets, Alex Clegg, John Turner, Eric Undersander, Wojciech Galuba, Andrew Westbury, Angel X Chang, et al. Habitat-matterport 3d dataset (hm3d): 1000 large-scale 3d environments for embodied ai. In *Conference on Neural Information Processing Systems Datasets and Benchmarks Track*, 2021.
- [53] Santhosh Kumar Ramakrishnan, Devendra Singh Chaplot, Ziad Al-Halah, Jitendra Malik, and Kristen Grauman. Poni: Potential functions for objectgoal navigation with interaction-free learning. In *Proceedings of the IEEE/CVF Conference on Computer Vision and Pattern Recognition*, 2022.
- [54] Ram Ramrakhya, Dhruv Batra, Erik Wijmans, and Abhishek Das. Pirlnav: Pretraining with imitation and rl finetuning for objectnav. *arXiv preprint arXiv:2301.07302*, 2023.

- [55] Ram Ramrakhya, Eric Undersander, Dhruv Batra, and Abhishek Das. Habitat-web: Learning embodied object-search strategies from human demonstrations at scale. In *Proceedings of the IEEE/CVF Conference on Computer Vision and Pattern Recognition*, 2022.
- [56] James Blake Rawlings, David Q Mayne, and Moritz Diehl. *Model predictive control: Theory, computation, and design*. Nob Hill Publishing Madison, WI, 2017.
- [57] Charles Richter, William Vega-Brown, and Nicholas Roy. Bayesian learning for safe high-speed navigation in unknown environments. In *Robotics Research*. Springer, 2018.
- [58] Mickaël Sauvée, Philippe Poignet, Etienne Dombre, and Estelle Courtial. Image based visual servoing through nonlinear model predictive control. In *Conference on Decision and Control*, 2006.
- [59] Manolis Savva, Abhishek Kadian, Oleksandr Maksymets, Yili Zhao, Erik Wijmans, Bhavana Jain, Julian Straub, Jia Liu, Vladlen Koltun, Jitendra Malik, et al. Habitat: A platform for embodied ai research. In *Proceedings of the IEEE/CVF International Conference on Computer Vision*, 2019.
- [60] Sanjana Srivastava, Chengshu Li, Michael Lingelbach, Roberto Martín-Martín, Fei Xia, Kent Elliott Vainio, Zheng Lian, Cem Gokmen, Shyamal Buch, Karen Liu, et al. Behavior: Benchmark for everyday household activities in virtual, interactive, and ecological environments. In *Conference on Robot Learning*, 2022.
- [61] Andrew Szot, Alexander Clegg, Eric Undersander, Erik Wijmans, Yili Zhao, John Turner, Noah Maestre, Mustafa Mukadam, Devendra Singh Chaplot, Oleksandr Maksymets, et al. Habitat 2.0: Training home assistants to rearrange their habitat. *Advances in Neural Information Processing Systems*, 2021.
- [62] V Tolani and et.al. Visual navigation among humans with optimal control as a supervisor. *IEEE Robotics and Automation Letters*, 2021.
- [63] Peter Trautman and Andreas Krause. Unfreezing the robot: Navigation in dense, interacting crowds. In *IEEE/RSJ International Conference on Intelligent Robots and Systems*, 2010.
- [64] Peter Trautman and Karankumar Patel. Real time crowd navigation from first principles of probability theory. In *International Conference on Automated Planning and Scheduling*, 2020.
- [65] J Van Den Berg and et.al. Reciprocal n-body collision avoidance. In *International Symposium on Robotics Research*, 2011.
- [66] Wouter van Toll, Fabien Grzeskowiak, Axel López Gandía, Javad Amirian, Florian Berton, Julien Bruneau, Beatriz Cabrero Daniel, Alberto Jovane, and Julien Pettré. Generalized microscropic crowd simulation using costs in velocity space. In *Symposium on Interactive 3D Graphics and Games*, 2020.
- [67] H Durrant Whyte. Simultaneous localisation and mapping (slam): Part i the essential algorithms. *Robotics and Automation Magazine*, 2006.
- [68] Erik Wijmans, Abhishek Kadian, Ari Morcos, Stefan Lee, Irfan Essa, Devi Parikh, Manolis Savva, and Dhruv Batra. DD-PPO: learning near-perfect pointgoal navigators from 2.5 billion frames. In *International Conference on Learning Representations*, 2020.
- [69] Fei Xia, Amir R Zamir, Zhiyang He, Alexander Sax, Jitendra Malik, and Silvio Savarese. Gibson env: Real-world perception for embodied agents. In *Proceedings of the IEEE/CVF Conference on Computer Vision and Pattern Recognition*, 2018.
- [70] Karmesh Yadav, Arjun Majumdar, Ram Ramrakhya, Naoki Yokoyama, Alexei Baevski, Zsolt Kira, Oleksandr Maksymets, and Dhruv Batra. Ovrl-v2: A simple state-of-art baseline for imagenav and objectnav. *arXiv preprint arXiv:2303.07798*, 2023.
- [71] Karmesh Yadav, Ram Ramrakhya, Santhosh Kumar Ramakrishnan, Theo Gervet, John Turner, Aaron Gokaslan, Noah Maestre, Angel Xuan Chang, Dhruv Batra, Manolis Savva, et al. Habitat-matterport 3d semantics dataset. In *Proceedings of the IEEE/CVF Conference on Computer Vision and Pattern Recognition*, 2023.

- [72] Wei Yang, Xiaolong Wang, Ali Farhadi, Abhinav Gupta, and Roozbeh Mottaghi. Visual semantic navigation using scene priors. In *International Conference on Learning Representations*, 2019.
- [73] Hongwei Yi, Chun-Hao P Huang, Shashank Tripathi, Lea Hering, Justus Thies, and Michael J Black. Mime: Human-aware 3d scene generation. In *Proceedings of the IEEE/CVF Conference on Computer Vision and Pattern Recognition*, 2023.
- [74] N Yokoyama and et.al. Benchmarking augmentation methods for learning robust navigation agents: the winning entry of the 2021 igibson challenge. In *IEEE/RSJ International Conference on Intelligent Robots and Systems*, 2022.
- [75] Martin Zimmermann, Minh Nhat Vu, Florian Beck, Anh Nguyen, and Andreas Kugi. Two-step online trajectory planning of a quadcopter in indoor environments with obstacles. *arXiv preprint arXiv:2211.06377*, 2022.